ChemPubSoc Europe

DOI: 10.1002/cctc.201501055

CHEMCATCHEM Communications

Investigation of Activated-Carbon-Supported Copper Catalysts with Unique Catalytic Performance in the Hydrogenation of Dimethyl Oxalate to Methyl Glycolate

Yuanyuan Cui, Bin Wang, Chao Wen, Xi Chen, and Wei-Lin Dai*[a]

Copper-based activated-carbon (AC)-supported catalysts were synthesized by a facile ammonia evaporation–impregnation method. Unlike the conventional Cu/SiO_2 catalyst, which showed highly catalytic selectivity towards ethylene glycol (EG) or EtOH, Cu/AC catalysts display unique selectivity to methyl glycolate (MG). The catalytic performance relies on the high content of surface Cu^+ species and the relatively large copper particles with moderate hydrogenation activity.

Synthesis of high-value-added alcohols from C1 blocks such as syngas and CO_2 has gained significant importance from a standpoint of fine chemical engineering and green chemistry. However, the direct synthesis of the target alcohols through hydrogenation of syngas or CO_2 involves quite complicated catalytic process and usually results in poor selectivity and complex product distribution, which greatly decreases the atom economy and the product yields. Thus, the indirect synthesis of alcohols with high catalytic selectivity and low energy consumption have aroused interest from the industrial community. One of the successful applications of the indirect synthesis of alcohols is the so-called coal to ethylene glycol (EG) project (CTEG), which contains two steps.[1] Firstly, high purity dimethyl oxalate (DMO) can be generated by the coupling of CO with nitrite esters; secondly, the hydrogenation of DMO to EG is required.[2]

In the hydrogenation of DMO process, another important product, methyl glycolate (MG), which is often in-situ hydrogenated to EG, can be obtained in the first step. MG is an essential intermediate for the synthesis of pharmaceutical products, fine chemicals, and perfumes. However, it is difficult to produce MG through the DMO hydrogenation process owing to thermodynamic factors that cause the further hydrogenation of MG to EG or EtOH to occur easily. Copper-based catalysts display superb catalytic performance in the DMO hydrogenation to EG or EtOH, and the highly dispersed copper species are considered as the key active sites.[2] Only when the catalyst becomes inactive does MG become prominent in the product distribution. It has been found that Ag-based catalysts can exhibit highly catalytic conversion of DMO as well as suppress the further hydrogenation of MG to other products. A MG yield of 92% was obtained at 493 K, 0.2 h^{-1} of DMO liquid hourly space velocity (LHSV) over 15 wt% Ag/SiO_2 catalyst. Furthermore, Ag catalysts with smaller Ag particle size display better catalytic performance compared with the catalysts with larger Ag particles.[3]

The design and fabrication of highly active and selective supported catalysts is of practical significance for industrial catalysis. Using the simplest ingredients and synthetic strategy in the catalyst fabrication process can greatly lower the cost and production time. It is very desirable that catalysts with superb catalytic performance can be synthesized with accessible raw materials and simple processes.

Activated carbon (AC) offers large versatility owing to its unique properties such as stability at low pH, the possibility of controlling porosity and surface chemistry, or easy recovery of precious metals. Many raw materials including coal, petroleum, and biomass can be used as the precursor of ACs, and their textural properties can be easily controlled by the preparation process.[4] AC-supported copper catalysts are widely used in hydrogenation reactions, NO reduction, aerobic oxidation of alcohols, and organic wastewater treatment process because of the high stability of the carbon support and the synergistic effects between the metal and support.[5]

In the present work, a series of coconut-based AC-supported copper catalysts were synthesized by a facile ammonia evaporation–impregnation method. The tight structure and the abundant functional groups on the surface make the AC an excellent support candidate for the copper-based catalysts.[6] Cu/AC catalysts with copper loading of 20 wt% were studied and named Cu/AC-*x*, where *x* denotes the calcination temperature (in K). The catalyst without heat treatment was donated as Cu/AC-non. Furthermore, the carbon nanotube (CNT)-supported copper catalyst, named Cu/CNT-673, was also synthesized for comparison. In our experiments, the Cu/AC catalysts display unique catalytic selectivity to MG similar to the Ag-based catalyst, which is quite different from the conventional Cu/SiO_2 catalysts.

All the carbon supports were functionalized with carboxyl and nitrate groups by nitric acid treatment before loading with active metals. The X-ray photoelectron spectroscopy (XPS), XRD, and FTIR results indicate that the treated AC supports afford more surface functional groups, which are conducive to the copper loading (see the Supporting Information, Figures S1–S4).

[a] *Y. Cui, B. Wang, C. Wen, X. Chen, Prof. Dr. W.-L. Dai*
Department of Chemistry and Shanghai Key Laboratory
of Molecular Catalysis and Innovative Materials
Fudan University
Shanghai, 200433 (P.R. China)
E-mail: wldai@fudan.edu.cn

Supporting Information for this article is available on the WWW under http://dx.doi.org/10.1002/cctc.201501055.

Table 1. Catalytic performances and physicochemical properties of the catalysts.

Catalyst	Conversion [%][a]	Selectivity to MG [%][a]	Selectivity to EG [%][a]	MG yield [%][a]	STY [$g\,g_{catal}^{-1}\,h^{-1}$][a]	BET [$m^2\,g^{-1}$]	D_{Cu}-Cal. [nm][c]	D_{Cu}-Re. [nm][c]	Cu^+/Cu^0[d]
Cu/AC-non	32	>99	–	32	0.058	9.6	–	35	0.62
Cu/AC-573	30	>99	–	30	0.054	15.4	33	36	0.64
Cu/AC-673	83	92	8	76	0.136	312	36	41	1.05
Cu/AC-773	47	>99	–	47	0.084	635	37	43	0.71
Cu/CNT-673	89	35	65	31	0.061(0.104)[b]	769	–	8	0.92

[a] Reaction conditions: $T = 493$ K, H_2/DMO = 120, $P_{H2} = 2.5$ MPa, LHSV = 0.18 h^{-1}, STY values to MG (STY represents the space–time yield of product for the catalysts: grams of product per gram of catalyst per hour ($g\,g^{-1}_{Catal}\,h^{-1}$)). [b] STY to EG shown in parenthesis. [c] Average Cu particle sizes calculated by XRD (Cal. = catalysts after calcination and Re. = catalysts after reduction). [d] Surface molar ratio of Cu^+/Cu^0 measured by XPS.

The catalytic performances of the catalysts are listed in Table 1. The DMO conversion with the Cu/AC-*x* catalysts increased with the calcination temperatures under N_2 atmosphere and the highest DMO conversion of 83% was obtained with Cu/AC-673. The catalyst calcined at 773 K showed lower DMO conversion. Generally, MG, the primary product of DMO hydrogenation, is easily further hydrogenated to the more stable product of EG owing to the high hydrogenation activity of the copper catalysts. Interestingly, Cu/AC-673 can be used to control the DMO hydrogenation process, stopping at the MG step with a selectivity to MG of 92% even when conversion of DMO was 83%. However, the conventional Cu/SiO_2 is more selective to EG (over 80%) under the same DMO conversion conditions.[1] The Cu/CNT-673 catalyst showed higher DMO conversion (89%, see Table 1) with MG selectivity of 35% and EG selectivity of 65%, indicating that using CNT as supports would result in more EG product. The highest space–time yield of MG could be obtained with the Cu/AC-673 catalyst, giving 0.136 $g\,g_{catal}^{-1}\,h^{-1}$.

The catalytic performance of Cu/AC-673 at different reaction temperatures is shown in Figure 1. The conversion of DMO was only 27% when the reaction temperature was 453 K and further increased to 83% when the temperature was increased to 493 K or higher. When the temperature was 533 K, the DMO conversion increased to 95%. Generally, MG is the main product when the conversion of DMO is low owing to the poor catalytic hydrogenation activity of the catalysts. Moreover, it has been reported that the high content of MG in the product distribution under low DMO conversion can easily result in the irreversible deactivation of the catalyst.[7] In addition, even when the reaction temperature was 533 K and the deep hydrogenation product EtOH becomes the main product with the Cu/SiO_2 catalyst, the selectivity to MG was still 45% over the Cu/AC-673 catalyst, suggesting that the AC-supported copper catalyst is more able to stabilize the DMO hydrogenation process to the MG product.

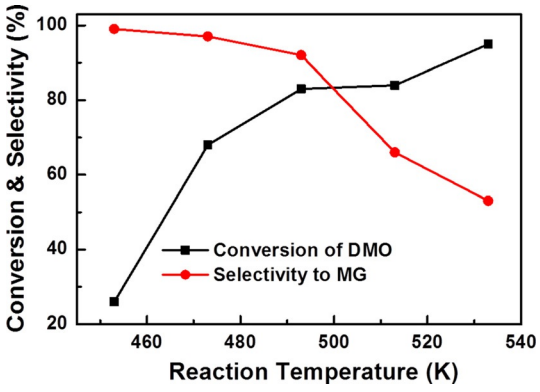

Figure 1. Catalytic performance of Cu/AC-673 at different reaction temperatures. Reaction conditions: H_2/DMO = 120, $P_{H_2} = 2.5$ MPa, LHSV = 0.18 h^{-1}.

The physicochemical properties of the catalysts are shown in Table 1. After loaded with copper species, the total specific surface areas of the catalysts decreased dramatically from 911 $m^2\,g^{-1}$ of the freshly treated AC support to 10 $m^2\,g^{-1}$ of the Cu/AC-non. During the preparation process, it was difficult for the cuprammonia species to infiltrate into the microporous structures of the AC supports; hence, copper species were mainly loaded on the surface of the supports during the ammonia evaporation–impregnation process. Thus, the porous structures of the AC supports were blocked, which further led to the drastic decrease of the specific surface area. The Cu/CNT catalysts calcined at higher temperatures showed much larger specific areas compared with the Cu/AC-non and Cu/AC-573; this was mainly due to the gradual decomposition of amorphous copper species into crystalline CuO and the growth of copper particles, which resulted in the increase of exposed pores. The CNT support contained meso and macro pores with a large specific area of 1032 $m^2\,g^{-1}$, which can uniformly disperse the copper species.

The XRD patterns of the calcined catalysts are shown in Figure S5(A) in the Supporting Information. The AC-supported and the Cu/AC-non catalysts showed no diffraction peaks, confirming the amorphous nature of these samples. After the catalysts were calcined under an N_2 atmosphere, the copper species were reduced by the carbon supports and the clear metallic copper diffraction peaks at 43.2, 50.4, and 74.1° can be observed. The copper particle size in the catalysts was calculated from the XRD results and are shown in Table 1. The copper particle size is 33.4 nm in Cu/AC-573 and further increased to 37.5 nm when the heat treatment temperature was increased to 773 K. However, there is no diffraction peaks in the XRD pattern of the Cu/CNT-673 catalyst, indicating that the copper species in the catalyst are highly dispersed as a result of the large specific area of the CNT support. The catalyst reduced at 573 K displayed much sharper metallic copper diffraction peaks compared with the calcined ones (see Figure S5(B) in

the Supporting Information). The copper particle sizes in the reduced Cu/AC-non and Cu/CNT-673 catalysts were 35 and 8 nm, respectively, indicating that the reduction process can also cause particle growth. In addition, copper particle sizes of the Cu/AC-*x* samples also displayed a small increase after reduction.

Clear copper particles could be observed in the TEM images of the reduced catalysts (see Figure S6 in the Supporting Information). The copper species in the Cu/AC-non (made without the calcination process) showed irregular dispersions on the AC support. However, the copper species in other catalysts, which had undergone the heat treatment process, presented spherical particles with different particle sizes and distributions depending on the calcination temperature. It was found that the spherical copper particle size increased with increasing calcination temperature, which was in accord with the XRD results. The copper species in the Cu/CNT-673 catalyst were also spherical in morphology with a particle diameter of 6 nm, suggesting that the large specific surface area is helpful for the copper dispersion. The calcination process under an N_2 atmosphere reduces some of the copper species into the metallic state and increases the copper particle size. However, the heat treatment can also stabilize the copper species and improve the copper distribution. The TEM and STEM images of the reduced Cu/AC-673 are shown in Figure 2. The spherical copper particles disperse uniformly on the AC support and the element mapping analysis also confirms the homogeneous dispersion of elemental copper.

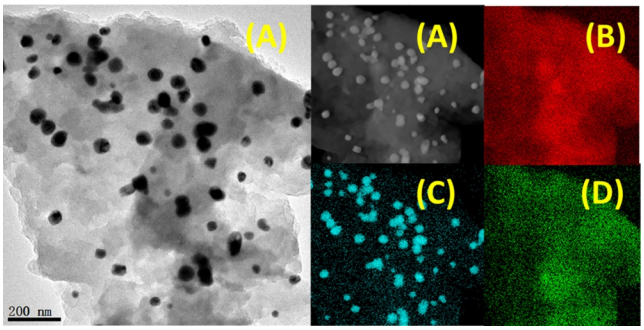

Figure 2. TEM (Left) and STEM (Right) images of the Cu/AC-673 catalyst (A). Mapping analysis of carbon (B), copper (C), and oxygen (D) in the Cu/AC-673 catalyst.

The FTIR spectra of the catalysts are shown in Figure 3. The clear peak at 1713 cm^{-1} was ascribed to C=O stretching. The peaks at 1520 and 1346 cm^{-1} from vibrational bands of the surface carboxyl groups could be observed, indicating the successful functionalization caused by the nitric acid treatment. Also, the C–H stretching vibration band of $-CH_3$ groups at 1383 cm^{-1} can be detected and does not change after copper is loaded onto the AC supports. However, the C=O vibration band of AC undergoes a blueshift to higher wavenumbers with increasing calcination temperatures of the Cu/AC-*x* catalysts, suggesting strong interaction between the copper species and the AC supports. Thus, the N_2 heat treatment not only

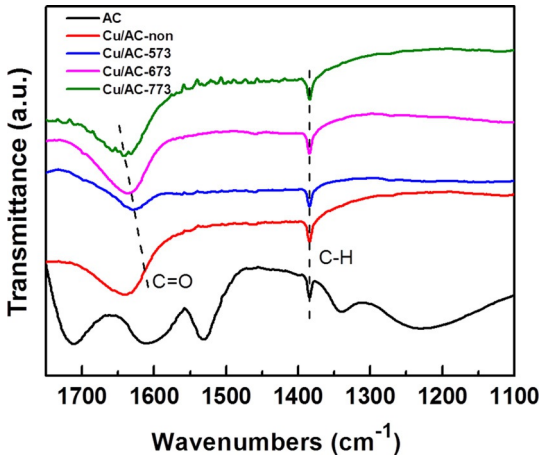

Figure 3. FTIR spectra of the various catalysts and AC support.

facilitated the copper reduction by the carbon support and helped to form the uniform distribution of copper particles, but also enhanced the metal–support interaction in the catalysts and further stabilized the copper species to avoid severe aggregation during H_2 reduction.

XPS was carried out to probe the surface chemical state of the catalysts. All the catalysts after reduction at 573 K showed Cu 2p peaks at 932.2 eV without any satellite peaks, indicating that the copper species were in the reduced state. However, further investigation by X-ray excited Auger electron spectroscopy (XAES) confirmed the existence of two overlapping Cu LMM Auger kinetic energy peaks centered at about 918.1 and 914.8 eV ascribed to Cu^+ and Cu^0, respectively, in the reduced catalysts (Figure 4). Deconvolution of the original Cu LMM peaks was thus carried out and the peak positions as well as their contributions extracted from the deconvolution are listed in Table 1. Cu/AC-non displayed the lowest molar ratio of Cu^+/Cu^0. The catalyst calcined at 573 K showed a slightly higher

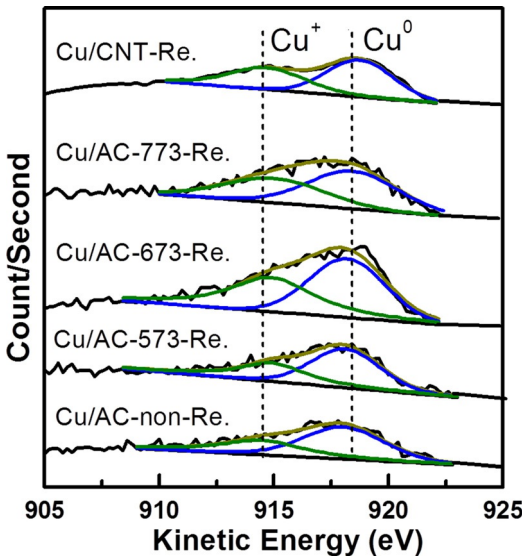

Figure 4. XAES spectra of the catalysts after reduction at 573 K.

Cu^+/Cu^0 value of 0.64. The Cu/AC-673 catalyst had the highest surface Cu^+ content with a molar ratio of $Cu^+/Cu^0 = 1.05$. Further increase in the calcination temperature decreased the Cu^+/Cu^0 distribution in the catalyst. As shown in Figure S7 in the Supporting Information, the intensity of Cu^+–CO on the Cu/AC-673 catalyst in the in-situ CO adsorption FTIR spectra is clearly enhanced compared with that on the Cu/AC-non catalyst, which illustrates that more Cu^+ species exist on Cu/AC-673. This result is in line with that from XAES.[8]

It is known that the strong interaction between the metal and the supports can stabilize the Cu^+ species in the reduced catalyst. The FTIR results indicated that the metal–support interactions in the catalyst increased with increasing calcination temperature; thus, Cu/AC-673 had higher Cu^+ content compared with the Cu/AC-573 catalyst. However, both the heat treatment under an N_2 atmosphere and pretreatment under H_2/Ar (vol%) at 573 K could cause the reduction of the copper species in the catalysts. With the increase in the calcination temperature, the carbon reduction effect has a greater influence on the copper reduction and further cause the deep reduction of the copper species to the Cu^0 state. Thus, the value of Cu^+/Cu^0 decreased in the Cu/AC-773 catalyst. In addition, Cu/CNT-673 also had the molar ratio of $Cu^+/Cu^0 = 0.92$, similar to the Cu/AC-673 ratio, which confirmed the calcination effect on the surface Cu^+/Cu^0 distribution.

It has been reported that hydrogenation of DMO takes place on the copper surface and the balanced Cu^+/Cu^0 sites are the main catalytic centers of the catalyst. The metallic Cu^0 species play important roles in the H_2 activation and the Cu^+ species could be considered as the stabilizer of the methoxy and acyl species, which are intermediates in DMO hydrogenation.[9] In addition, Cu^+ sites could function as electrophilic or Lewis acidic sites to polarize the C=O bond through the electron lone pair in oxygen; thus, improving the reactivity of the ester group in DMO. Based on Gong's study, the turnover frequency (TOF) of the catalysts in the DMO hydrogenation process decreased with increasing $Cu^0/(Cu^0+Cu^+)$ value in the range of 0.33–1.00.[10] The $Cu^0/(Cu^0+Cu^+)$ values of the Cu/AC-*x* catalysts in the present work are in the range of 0.49–0.62. Cu/AC-673, with the lowest $Cu^0/(Cu^0+Cu^+)$ distribution, displayed the highest catalytic activity, strongly confirming the crucial effect of the Cu^+/Cu^0 balance. Our results are also consistent with Huang's study in which the MG yield reached the maximum when $Cu^+/(Cu^0+Cu^+)$ reached its summit.[11]

Cu/CNT-673, which has a similar $Cu^0/(Cu^0+Cu^+)$ value, exhibited higher DMO conversion and selectivity to EG compared with Cu/AC-673. The XRD calculation and TEM images revealed the much smaller copper particle size in the reduced Cu/CNT-673 catalyst. It is known that smaller metal particles exhibit higher hydrogenation activities compared with larger ones owing to the large specific areas and low activation energies.[12] Thus, the copper particles in Cu/CNT-673 are expected to exhibit higher catalytic activities compared with those in Cu/AC-673. As a result, the higher hydrogenation activity of Cu/CNT-673, which displayed higher DMO conversion, can further convert the MG intermediate into EG.

The unique catalytic performance of Cu/AC-673, which showed relatively high DMO conversion and much higher selectivity to MG compared with other Cu/AC-*x* catalysts, is attributed to the balance between the Cu^+/Cu^0 species. Furthermore, the relatively repressed hydrogenation activity caused by the large copper particles also plays a significant role in preventing further hydrogenation of MG to EG. The Cu/AC-673 catalyst can run stably at 493 K with a DMO conversion of 83% and yield of MG higher than 75% without any deactivation even after 120 h time on stream (see Figure S8 in the Supporting Information), which indicates analogous stability with the reported Ag/SiO_2 catalyst.[3] XPS examination of the spent Cu/AC-673 catalyst revealed that the chemical state of the copper species did not change compared with the freshly reduced one, confirming the stabilization effect caused by the calcination process under an N_2 atmosphere (see Figure S9 in the Supporting Information).

In summary, unlike the conventional Cu/SiO_2 catalyst, the Cu/AC-673 catalyst displayed a unique catalytic performance with high selectivity to MG under relatively high DMO conversion. The copper species in the catalyst were reduced by the AC support during the calcination process, which also played an important role in stabilizing the copper particles. The high yield to MG is attributed to the moderate hydrogenation activity and high molar ratio of Cu^+/Cu^0. The ammonia evaporation–impregnation method, which can generate homogeneously dispersed copper-based catalysts, could also be used to synthesize other highly active supported catalysts.

Experimental Section

Catalyst preparation

All the carbon supports were treated with concentrated nitric acid at 353 K for 24 h to functionalize the supports with carboxyl and nitro groups before loading with copper species. Detailed characterizations of the functionalized supports are shown in the Supporting Information.

The Cu/AC-*x* catalysts with 20 wt% copper loading were prepared by a facile ammonia evaporation–impregnation method. Firstly, $Cu(CH_3COO)_2{\cdot}H_2O$ (3.75 g) was dissolved in deionized water (200 mL). Then, approximately 20 mL of aqueous ammonia (25 wt%) was added to the above solution and the pH was adjusted to 11.0. After that, the pretreated AC support (4.8 g) was added into the solution. The as-obtained suspensions was stirred for 4 h at room temperature, and then the temperature was increased to 363 K until the solvent had evaporated completely to decompose the cuprammonia species. Finally, the catalyst precursors were calcined under an N_2 flow at different temperatures. The catalysts were named Cu/AC-*x* where *x* stands for the calcination temperature. The catalyst without calcination was named Cu/AC-non. Cu/CNT-673 catalyst with 20 wt% copper loading and CNT support was synthesized by the same method as Cu/AC-673. All the catalyst were pelletized, ground to 40–60 meshes, and went through further hydrogen treatment at 573 K for 4 h with a ramping rate of 2 K min^{-1} from room temperature for pre-activation before the catalytic tests.

Catalytic activity measurements

The catalytic activity tests were conducted by using a fixed-bed micro-reactor. Typically, the catalyst (0.8 g, 40–60 meshes) was packed into a stainless steel tubular reactor (i.d. = 5 mm) with a thermocouple inserted into the catalyst bed. Catalyst activation was performed at 573 K for 4 h with a ramping rate of 2 K min^{-1}. After cooling to the reaction temperature, DMO (15 wt%, purity > 99%) in methanol and H_2 were fed into the reactor at a H_2/DMO molar ratio of 150 and a system pressure of 3.0 MPa. The reaction temperature was first set at 493 K and the room-temperature LHSV of DMO was set at 0.2 h^{-1} for the initial 6 h to achieve steady-state reaction. After the collected reaction liquid was released, the room-temperature LHSV of DMO ranged from 0.2 to 4.0 h^{-1}. The products were condensed, and analyzed on a gas chromatograph (Finnigan Trace GC ultra) fitted with an HP-5 capillary column and a flame ionization detector (FID). The corresponding data were collected at an interval of 30 min after the reaction attained a steady state.

Acknowledgments

We would like to thank the Major State Basic Resource Development Program (Grant No. 2012CB224804), NSFC (Project 21373054, 21173052), and the Natural Science Foundation of Shanghai Science and Technology Committee (08DZ2270500) for financial support.

Keywords: activated carbon · copper · dimethyl oxalate · hydrogenation · methyl glycolate

[1] H. Yue, Y. Zhao, X. Ma, J. Gong, *Chem. Soc. Rev.* **2012**, *41*, 4218 – 4244.
[2] a) H. Yue, X. Ma, J. Gong, *Acc. Chem. Res.* **2014**, *47*, 1483 – 1492; b) E. Jin, Y. Zhang, L. He, H. G. Harris, B. Teng, M. Fan, *Appl. Catal. A* **2014**, *476*, 158 – 174.
[3] A. Yin, X. Guo, W. Dai, K. Fan, *Chem. Commun.* **2010**, *46*, 4348 – 4350.
[4] L. Jin, H. Si, J. Zhang, P. Lin, Z. Hu, B. Qiu, H. Hu, *Int. J. Hydrogen Energy* **2013**, *38*, 10373 – 10380.
[5] a) R. S. Rao, R. T. K. Baker, M. A. Vannice, *Catal. Lett.* **1999**, *60*, 51 – 57; b) C. Márquez-Alvarez, I. Rodriguez-Ramos, A. Guerrero-Ruiz, *Carbon* **1996**, *34*, 1509 – 1514; c) G. Yang, W. Zhu, P. Zhang, H. Xue, W. Wang, J. Tian, M. Song, *Adv. Synth. Catal.* **2008**, *350*, 542 – 546; d) X. Hu, L. Lei, H. P. Chu, P. L. Yue, *Carbon* **1999**, *37*, 631 – 637.
[6] M. Al Bahri, L. Calvo, M. A. Gilarranz, J. J. Rodriguez, F. Epron, *Appl. Catal. B* **2013**, *138*, 141 – 148.
[7] C. Wen, Y. Cui, X. Chen, B. Zong, W. L. Dai, *Appl. Catal. B* **2015**, *162*, 483 – 493
[8] Y. N. Wang, X. P. Duan, J. W. Zheng, H. Q. Lin, Y. Z. Yuan, H. Ariga, S. Takakusagi, K. Asakura, *Catal. Sci. Technol.* **2012**, *2*, 1637 – 1639.
[9] Z. He, H. Lin, P. He, Y. Yuan, *J. Catal.* **2011**, *277*, 54 – 63.
[10] J. Gong, H. Yue, Y. Zhao, S. Zhao, L. Zhao, J. Lv, S. Wang, X. Ma, *J. Am. Chem. Soc.* **2012**, *134*, 13922 – 13925.
[11] Y. Huang, H. Ariga, X. Zheng, X. Duan, S. Takakusagi, K. Asakura, Y. Yuan, *J. Catal.* **2013**, *307*, 74 – 83.
[12] a) Z. Yuan, L. Wang, J. Wang, S. Xia, P. Chen, Z. Hou, X. Zheng, *Appl. Catal. B* **2011**, *101*, 431 – 440; b) X. Zhou, W. Xu, G. Liu, D. Panda, P. Chen, *J. Am. Chem. Soc.* **2010**, *132*, 138 – 146.

Received: September 24, 2015
Revised: October 28, 2015
Published online on December 16, 2015